CONF-8808141--8

LIQUID GALLIUM COOLING OF SILICON CRYSTALS IN HIGH INTENSITY PHOTON BEAM*

R. K. Smither and G. A. Forster
Argonne National Laboratory, Argonne, IL 60439 USA

D. H. Bilderback, M. Bedzyk, K. Finkelstein, C. Henderson, and J. White
Cornell University, Ithaca, NY 14853

and

L. E. Berman, P. Stefan, and T. Oversluizen
Brookhaven National Laboratory, Upton, NY 11973

November 1988

CONF-8808141--8

DE89 005875

This paper submitted to the proceedings of the 3rd International Conference on Synchrotron Radiation Instrumentation: SRI-88, held in Tsukuba, Japan, August 29-September 2, 1988.

*This work supported by the U.S. Department of Energy, BES-Materials Sciences, under contract no. W-31-109-ENG-38.

LIQUID GALLIUM COOLING OF SILICON CRYSTALS IN HIGH INTENSITY PHOTON BEAM*

R. K. Smither and G. A. Forster
Argonne National Laboratory, Argonne, IL 60439 USA

D. H. Bilderback, M. Bedzyk, K. Finkelstein, C. Henderson, and J. White
Cornell University, Ithaca, NY 14853 USA

L. E. Berman, P. Stefan, and T. Oversluizen
Brookhaven National Laboratory, Upton, NY 11973 USA

ABSTRACT

The high-brilliance, insertion-device-based, photon beams of the next generation of synchrotron sources (Argonne's APS and Grenoble's ESRF) will deliver large thermal loads (1 kW to 10 kW) to the first optical elements. Considering the problems that present synchrotron users are experiencing with beams from recently installed insertion devices, new and improved methods of cooling these first optical elements, particularly when they are diffraction crystals, are clearly needed. A series of finite element calculations were performed to test the efficiency of new cooling geometries and new cooling fluids. The best results were obtained with liquid Ga metal flowing in channels just below the surface of the crystal. Ga was selected because of its good thermal conductivity and thermal capacity, low melting point, high boiling point, low kinetic viscosity, and very low vapor pressure. Its very low vapor pressure, even at elevated temperatures, makes it especially attractive in UHV conditions. A series of experiments were conducted at CHESS in February of 1988 that compared liquid gallium cooled silicon diffraction crystals with water cooled crystals. The six pole wiggler beam was used to perform these tests on three different Si crystals, two new cooling geometries

*This work supported by the U.S. Department of Energy, BES-Materials Sciences, under contract no. W-31-109-ENG-38.

and the one presently in use. A special high pressure electromagnetic induction pump, recently developed at Agronne, was used to circulate the liquid gallium through the silicon crystals. In all experiments, the specially cooled crystal was used as the first crystal in a two crystal monochromator. An infrared camera was used to monitor the thermal profiles and correlated them with rocking curve measurements. A second set of cooling experiments were conducted in June of 1988 that used the intense, well collimated beam from the newly installed ANL/CHESS undulator. Tests were performed on two new Ga cooled Si crystals and compared with the standard CHESS water-cooled Si crystal. One of the crystals had cooling channels at two levels in the crystal that allowed one to actively control the the shape of the crystal surface. Both crystals shown major improvements over the standard water-cooled CHESS crystal.

INTRODUCTION

The high-brilliance, insertion-device-based, X-ray beams of the next generation of synchrotron sources, Argonne's Advanced Photon Source (APS), the European Synchrotron Radiation Facility (ESRF), and the Japanese Synchrotron Project will deliver large thermal loads to various components in the beam lines. The first optical element will often absorb the full heat of these intense X-ray beams which will range in power from 1 kW to 20 kW. The increased collimation of the next generation sources will increase the seriousness of these problems still further. Hence, improved methods of cooling the first optical elements, particularly when they are diffraction crystals, are clearly needed.

Liquid metal cooling has worked well in other high heat load applications, particularly in high temperature reactors, and appeared to be a

good solution in this case as well. After consulting the large bank of information on liquid metals available at ANL, liquid gallium was chosen as the most promising cooling fluid.[1] Liquid gallium has good thermal conductivity and thermal capacity, a low melting point, and a high boiling point. Its very low vapor pressure, even at elevated temperatures, makes it especially attractive in UHV conditions. This turned out to be a good choice because in the first tests of the use of liquid gallium as a cooling fluid for cooling diffraction crystals in a synchrotron beam, the new approach increased the usable flux from the first monochromator by factors of three to five and made it possible to use the full beam intensity in their experiments for the first time.

PRESENT COOLING PROBLEMS

An example of the heat load problems encountered at operating synchrotron facilities is the two crystal monochromator used on the A2 beamline at CHESS. This monochromator intercepts one third of the beam (350 W) from the six pole electromagnetic wiggler. The out put of this monochromator increased with increasing beam current until the current approached 10 mA and then leveled off giving no further improvement as the beam was increased to 70 mA. A plot of the out put of the monochromator verses electron beam current is shown in Fig. 1. Thus a factor of seven in intensity was lost due to the distortion of the crystal by the heat load. When this problem was analyzed in detail it was found that the distortion of the first crystal spreads the diffracted beam in both angle and energy so that only some of the beam had the right incident angle and energy to be diffracted by the second crystal of the monochromator (see Fig. 2). The observed rocking curves, taken by rotating the second crystal in Fig. 2, are given in Fig. 3. The different curves are

labeled with the corresponding current (electrons) in the storage ring. High temperatures and large distortions occur at small values of the ring current because of the long path that the heat must travel to exit the crystal.

SURFACE TEMPERATURES AND CRYSTAL DISTORTIONS

The temperature of the surface of the diffraction crystal (T_1) relative to the initial temperature of the cooling fluid (Tf) is given by equation (1)

$$T_1 = \Delta T_{12} + \Delta T_{23} + \Delta T_3 + T_f \qquad (1)$$

where "ΔT_{12}" is the temperature difference across the crystal, "ΔT_{23}" is the temperature difference between the inside crystal surface and the cooling fluid, and "ΔT_3", is the change in temperature of the cooling fluid relative to it's initial input temperature, "T_f".

These temperature distributions generate three different kinds of distortions in the diffraction crystal. The first two are illustrated in Fig. 4. First, there is the over all bending or bowing of the crystal caused by the thermal gradients in the crystal, second, there is the thermal bump (shaded area) that is caused by the expansion of the crystal perpendicular to the surface and third, there is the change in the crystal lattice spacing through thermal expansion caused by the increase in the surface temperature of the crystal. These effects varies over the surface of the crystal, following the variation in thermal loading of the surface. In the case of a crystal of uniform thickness, heated uniformly on the top surface and cooled uniformly on the bottom surface, the bowing of the surface is given by equations (2-4),

$$R = D \,/\, \alpha \Delta T_{12} = k/\alpha Q \qquad (2)$$

$$\Delta T_{12} = T_1 - T_2 = QD \,/\, k \qquad (3)$$

$$\Delta \theta_b = \Delta x \; k \,/\, \alpha \, Q \qquad (4)$$

where "D" is the thickness of the crystal, "R" is the radius of curvature of the crystal generated by "Q", the heat load per unit area, "α" is the thermal coefficient of expansion, "k" is the thermal conductivity, "ΔT_{12}" is the temperature difference between the top (T_1) and bottom surface (T_2) and "$\Delta\theta_b$" is the change in angle or angular error that occurs as one moves a distance "Δx" along the surface of the bowed crystal. The value of "R" is independent of the thickness of the crystal "D" and depends only on the parameters, "k" and "α", of the crystal material and the heat flow, "Q", through the crystal. If "ΔT_{12}" is 50°C and "D" is 1.5 cm and "α" is 3×10^{-6} per degree C (for silicon), then "R" = 100 m. This corresponds to heat flow through the crystal of Q = 50 watts per cm^2, from equation (2), where "k" = 1.5 watts per cm per °C (for silicon). In this example, a distance of 1 cm along the face of the bowed crystal corresponds to a change in angle, and thus an angular error, of 20.4 arc sec.

If heat is added non-uniformly to the front face of the crystal, varying from zero to "Q" at the center of the beam, then the height (H) of the thermal bump is given by equation (5).

$$H = \alpha\ \Delta T_{12}\ D/2 \cong \alpha\ Q\ D^2/2k \qquad (5)$$

where "Q" is now the heat load at the center of the thermal bump. Note that the value of "H" is proportional to "D^2" and thus very sensitive to the thickness of the crystal. If the shape of the thermal bump is Gaussian with a FWHM of "2X", then the maximum slope and thus maximum angular error, "$\Delta\theta_{max}$", is given by equation (6)

$$\Delta\theta_{max} = 1.432\ (H/2X) = 1.432\ (H/FWHM) \qquad (6)$$

Using the above parameters and a "2X" = 2 cm, "$\Delta\theta_{max}$"= 16.4 arc sec. This is similar to the angular error "$\Delta\theta_b$" = 20.4 arc sec obtained by moving 1 cm along the surface of the bowed crystal mentioned above. This thermal-bump

angular error increases the incident angle of the photon beam on the upstream side of the thermal bump and decreases it on the down side of the bump, giving a maximum spread of angular errors of 32.8 arc sec.

The third type of distortion produced by the photon beam is the change in the spacing between crystalline planes with the increase in the surface temperature of the crystal. This change in spacing is equivalent to a change in the diffraction angle, "$\Delta\theta_d$", which is given by equation (7),

$$\Delta\theta_d = -\alpha\ \Delta T \tan\theta \cong -\alpha\ \Delta T\ \theta \text{ (small angle approx)} \qquad (7)$$

where "ΔT" is the variation in the temperature of the crystal surface. A 50°C temperature rise will change the lattice spacing by "$\alpha\ \Delta T$" = 1.5×10^{-4} and give an equivalent angular error of "$\Delta\theta_d$" = 3.0 arc sec for a 20 keV photon beam diffracted by (111) Si planes and "$\Delta\theta_d$" = 7.5 arc sec for an 8 keV photon beam. The d-spacing errors, "$\Delta\theta_d$", are all in one direction so they cause an asymmetry in the overall angular error relative to the center of the photon beam. The "$\Delta\theta_d$" errors are 5 to 10 times less than the other two mentioned above and are comparable to the Darwin widths for these cases so they result in only a modest increase in the angular errors. These estimates of the relative importance of the different distortions are in agreement with the measurements of W. Edwards, et al.[2]

HEAT TRANSFER TO THE COOLING FLUID

The temperature difference, "ΔT_{13}", between the surface of the crystal and the cooling fluid (see Fig. 4) is made up of two parts as shown in equation (8).

$$\Delta T_{13} = \Delta T_{12} + \Delta T_{23} \qquad (8)$$

The first part, "ΔT_{12}", is the same temperature difference that was discussed above and corresponds to the temperature difference across the crystal in

Fig. 4. The second part , "ΔT_{23}", is the temperature difference between the inner wall of the crystal (T_2) and the cooling fluid (T_3). This is given by equation (9,10)[3]

$$\Delta T_{23} = Q/h \tag{9}$$

$$h = A_1 k/d + A_2 \, (k^{0.6} C_v^{0.4}/d^{0.2} \nu^{0.8}) V^{0.8} \tag{10}$$

where "Q" is the heat load per unit area and "h" is the heat transfer coefficient at the solid -liquid interface. "h" consists of two parts, the first of which involves the thermal conductivity "k" divided by "d", the effective hydraulic diameter, which reflects the size and shape of the cooling channels. The second term includes the ratio of "k" and "d" and in addition, C_v is the specific heat per unit volume, V is the velocity and ν is the kinetic viscoity of the cooling fluid. "A_1" and "A_2" are constants. The second term contains the velocity of the cooling fluid and therefore, becomes the dominate term at high flow rates while the first term dominates at low flow rates.

FINITE ELEMENT ANALYSIS

A series of "finite element " calculations were made to determine the best cooling geometry for use with the first diffraction crystal of a two crystal monochromator.[1] The first set of calculations obtained the distribution of temperatures through out the crystal when a heat load was applied. The second set, based on the first set, determined the resulting distortion of the crystal surface. The best results (least distortion) were obtained when the cooling fluid was circulated through channels just below the surface of a thick crystal. This reduced the effective value of "D", the distance between the diffraction surface of the crystal and the cooling fluid surface, to a minimum value and thus the angular errors generated by both the

thermal bump and those from the change in crystal lattice spacing, to a minimum (see equations 5, 6 and 7). The angular errors from the bowing distortion are reduced by using a crystal that has considerable depth, "L", below the cooling channels. When the dimensions of the cooling channels are small compared to the thickness of the crystal and "L" is large compared to "D", the reduction in the bowing errors is roughly proportional to $(D/L)^2$.

The equations for the different distortions given in the previous section are only approximations for the more complicated crystal geometries with cooling channels in the crystal. The effective value of "D" is different for equation (2) than it is for equation (4). In equation (2) the effective value of "D" is less than the minimum distance between the surface and the cooling channel because of the fin cooling effect and in equation (4) the effective value of "D" is greater than because the thermal gradient expends down into the fine area between channels, increasing the depth over which the crystal expands. The finite element analysis is most useful for the calculations for these cases with complex geometries.

CHOICE OF GALLIUM AS THE COOLING FLUID

The finite element analysis was also used to compare different cooling fluids[1] and made it quite clear that liquid metals were more efficient cooling fluids than water under almost all conditions. Ga was the most attractive of the liquid metals for synchrotron applications.[1] Table I compares the physical properties of liquid gallium with water. These physical properties directly effect the value of "h" used to calculate "ΔT_{23}" in equation (8). The biggest difference between the two cooling fluids comes in the values for "k" their thermal conductive. The high value of "k" for gallium makes both terms in equation (8) important while the very low value of "k" for water

makes the first term very small and the second term small as well until the fluid velocity (V) becomes large. A plot of "h" verses flow rates for liquid gallium (upper curve) and water (lower curve) in 0.5 cm diameter channels, is given in Fig. 5. One can see immediately from this plot why gallium is the preferred cooling fluid. The value of "h" for gallium starts out much higher than that for water because of gallium's much larger thermal conductivity (k) and remains higher at all flow rates because the coefficient on the second term is also larger for gallium that for water.

ELECTROMAGNETIC INDUCTION PUMP

The liquid gallium is pumped through channels just below the surface of the silicon crystal with an electromagnetic induction pump developed at the Argonne National Laboratory for this purpose.[1] The heart of the pump is a modified 5 hp, 3 - phase, induction motor, where the central rotor has been machined down to make room for the spiral stainless steel tube that fits into the widened gap between the now fixed rotor and the stator. The rotating magnetic field in the 3-phase motor induces a current to flow down one side of the coil and up the other side. The interaction of the moving magnetic field and the current generates a continuous, non-pulsating force on the liquid gallium that produces the pumping action. The pump develops a static head pressure of 45 psi and can pump 3 gpm through a typical cooling system with silicon crystal a mounted a few feet away from the pump. The essential feature and the new development in this pump is its high pressure head and its smooth, non-pulsating flow. Most liquid metal pumps are low pressure devices. The high pressure is needed to push the liquid gallium through the crystal cooling system at the high flow rates (1-3 gpm) needed to obtain optimum cooling of the crystals.

COOLING EXPERIMENTS WITH WIGGLER BEAMS

Water is used as the cooling fluid in most present day synchrotron facilities but as mentioned above, is not efficient enough to cool some of the more recently developed beams for newly installed wigglers and undulators and will encounter even more difficulties when trying to cool the insertion device beams at the next generation of synchrotrons (APS, ESRF, etc.).[1] This makes it very important to start investigating new cooling fluids and new cooling geometries.

A set of experiments were performed in February 1988, using the radiation from the six-pole wiggler at CHESS, the synchrotron facility at Cornell. A comparison was made between the performance of three silicon crystals as x-ray monochromators cooled with either liquid gallium or water. The two gallium cooled Si crystals had 5 mm dia. cooling channels drilled through them just below the diffraction surface (111). One measured 7.5 cm x 7.5 cm (diffraction area) by 1.5 cm thick and had five cooling channels who's center lines were 5 mm below the surface. The second channel-cooled crystal measured 10 cm long in the direction of the beam, 3.8 cm wide and 2.5 cm thick, with three 5mm dia. cooling channels with centers 5mm below the surface. The third crystal used in these tests was the Si crystal that is normally used in the CHESS monochromator on beamline A2. This crystal has the same dimensions as the crystal with three cooling channels describe above but was cooled on three sides with water cooled copper blocks thermally coupled to the crystal with an indium-gallium eutectic interface. Tests were also run on the three channel crystal with water cooling. The cross sections of these three crystals is shown in Fig. 6.

In all tests, the specially cooled crystal was used as the first crystal in a two crystal monochromator and received the full power from the wiggler

source. The wiggler is 18.5 m from the specially cooled crystal which diffracts the analyzed photon beam upward. A second crystal, located a few cm away, diffracts the beam a second time, returning it to the horizontal direction. The doubly diffracted beam is then analyzed in a hutch located 7.5 m farther down stream. An infrared camera was used to monitor the thermal profile of the photon beam on the crystals. This made it possible to measure the height and shape of the thermal profile with different stored ring currents in the synchrotron and when carbon absorbers with different thickness were placed in the photon beam. Fig. 7 shows the thermal profile obtained with the three different crystals with 46 mA in the storage ring and compares the thermal profiles of one of the crystals when cooled with both gallium and water. The highest profile is that for the Standard CHESS crystal with side cooling. The next three are for the 3-channel crystal. Water was used as the cooling fluid for the higher of the three and gallium for the next lower two. The lowest thermal profile is for the 5-channel crystal with gallium cooling. The improved cooling of this last case comes from a better cooling geometry. These measurements were correlated with rocking curve measurements at 8 and 20 keV, made by rotating the second crystal in the monochromator and with scanning slit measurements of the beam profile. At low photon beam intensities corresponding to low electron beam currents in the storage ring, almost all of the photons that are diffracted by the first crystal are also diffracted by the second crystal.

A comparison of the rocking curves obtained for the different crystals with different cooling fluids is shown in Fig. 8. The lower dashed curve corresponds to the Standard CHESS side-cooled crystal that was discussed in the section on "Present Cooling Problems". The use of water cooling near the surface in the 3-channel crystal reduced the distortion in the crystal by

about 36 percent, with a corresponding increase in the peak intensity. This case is shown in Fig. 8 as the higher dashed curve. When Ga was used for the cooling fluid in this crystal, the rocking curve becomes narrower and higher (lower solid line). When the Ga flow rate in the crystal was increased to 1.33 gpm, the distortion was reduced by 30 percent. The best results were obtained with the Ga-cooled 5-channel crystal (upper solid curve) which increased the peak intensity by a factor of 3 to 5 (depending on the energy and cooling fluid flow rate) over that obtained with the side-cooled crystal. Fig. 9 shows the rocking curve for the 5-channel crystal when different carbon absorbers are put into the photon beam. The observed intensity with the full beam (46 mA) is 5 percent less the predicted value, so the loss of intensity with the full beam is almost within our experimental error. This suggests that the intensity of the beam could be appreciable higher before major distortion occurs that would limit the intensity of the beam diffracted by the second crystal. A detailed analysis of the thermal profiles observed for the Argonne crystal and comparison with the calculated results suggests that the channels could be closer to the surface by a factor of 2.5 if the channels were made smaller. This would reduce the height of the thermal profile and the amount of distortion of the crystal surface by a similar factor of 2.5 for the bowing errors and a factor of 6.25 for the thermal bump errors. This would allow one to increase the intensity of the primary beam by a similar factor of 2.5 without serious losses in the final diffracted beam.

COOLING EXPERIMENTS WITH UNDULATOR BEAMS

A second set of experiments were performed at CHESS in June of 1988. They used the intense photon beams generated by the newly installed ANL/CHESS

undulator.[4,5] The experimental setup was the same as that used in the previous cooling experiments with a distance from the undulator to the first crystal of 18.5 m and the detector station located 7.5 m farther down stream. As before, a electromagnetic induction pump was used to circulate liquid gallium through channels in the first crystal. Two new silicon crystals with new cooling geometries were tested and compared to the performance of the standard CHESS side-cooled crystal.[6] The cross section and thermal foot print of the first crystal is shown in Fig. 10. It has a very thin top layer, 0.76 mm, cooled by slots 2.33 mm wide and supported by fins or ribs 0.80 mm wide. This upper structure was fabricated as a single piece and glued onto a 19.05 mm thick base crystal.[6] It was designed to test the dependence of the crystal distortions on the thickness of the top layer. (See equations 4 and 6) A plot of the peak temperature of the thermal bump verses flow rate of the liquid gallium for different synchrotron beam currents is given in Fig. 11. At first, the peak temperatures drop rapidly as the flow changes from laminar to turbulent and the distribution of the flow in the channels becomes more uniform. In this region equation (9) is not a good approximation for "ΔT_{23}", the temperature difference at the solid-liquid interface. This is also the region where the thermal gradients extend down into the fin structure. This gives rise to an increase in the effective value of "D", and thus an increase in both the bowing and the thermal bump. Part of the strong variation in peak temperature of the thermal profile will come from these effects. For flow rates of 0.6 gpm and above, the flow pattern stabilizes and equation (9) is a good approximation for "ΔT_{23}". In this region the peak of the thermal profile shows an almost linear dependence on flow rate and agrees well with the "$V^{0.8}$" dependence for the value of "h" given in equation (9), which leads to a similar dependence for the peak

temperature of the thermal profile. All curves in Fig. 11 are decreasing with increasing flow rates so considerable improvement can be made by further increase in the flow rate. The peak temperature will approach a constant temperature given by equation 3, at high flow rates. This corresponds to the temperature difference across the top layer of the crystal, "ΔT_{12}". This lower limit for the 70 mA curve is about 18°C and for the lowest curve at 30 mA is about 8°C. Doubling the flow rate to 3.2 gpm would reduce the maximum temperature for the 70 mA curve from 68°C to 43°C and for the 30 mA curve from 25°C to 16°C.

The second gallium cooled crystal tested was 7.7 cm wide, 7.7 long and 2 cm thick, with 2 sets of 5 cooling channels, 5mm in dia. The center line of the first set of channels were 5 mm below the surface giving a minimum distance to the surface of the crystal of 2.5 mm. The second set were 15 mm below the surface. The cross section and thermal foot print for this crystal are shown in Fig. 12. The energy of the diffracted beam is 8 keV and the incident angle about 13 degrees. The thermal profile is narrower than it was for the slotted crystal as would be expected because the beam strikes the crystal more perpendicular to the surface. The thicker top layer of the silicon crystal and the smaller thermal footprint will generate a larger "ΔT_{12}". This will be reduced by some 10 to 20 percent by the more efficient fine-cooling of the much thicker rib structure but the "ΔT_{12}" will still be much larger. The larger "ΔT_{12}" will generate larger distortions of the crystal and thus wider rocking curves. Fig. 13 compares the width of the rocking curves of the two gallium cooled crystals as a function beam current and gallium flow rate. The upper two curves are for the 10-hole dual level cooling-channel crystal. The upper curve is the case for 8 keV diffraction with a gallium flow of 0.62 gpm and the lower curve for 13 keV diffraction

with 1.22 gpm flow. The lower slope of the second curve reflects both the larger thermal footprint and thus lower heat load per unit area of the more spread out beam of the 13 keV diffraction case and the more efficient cooling of the higher gallium flow rate. Higher flow rates will lower both of these curves. The lower four curves are for the slotted crystal with the very thin top layer, with gallium flow rates that vary from 0.26 gpm to 1.62 gpm. Again, further improvement is possible with increased flow rates. The almost linear dependence of these curves on electron beam current makes it possible to extrapolate these curves to higher beam currents that will be available in the future. The curves for the 10-channel crystal start out higher than those for the slotted crystal. This is a result of the slightly mosaic structure of 10-channel crystal.

Fig. 14 is a plot of the count rate of the photon beam after it is diffracted by the second crystal in the two crystal monochromator as a function of the electron beam current in the synchrotron storage ring and gallium flow rate. If there were no distortion in the diffraction crystals these curves would be straight lines (see dashed curve). Again we see consider improvement with increased gallium flow and the better results for the slotted crystal with its much thinner top layer. It is interesting to note that at low flow rates, 0.26 gpm, the performance of the slotted crystal is very similar to the high flow case of the 10-hole crystal with its much thicker top layer. This is believed to be due to the poorer heat transfer in the slotted crystal at low flow rates that comes from the poorer flow pattern, less flow at the ends of the narrow slots. This poorer cooling of the fins, extends the thermal gradient down into the fin structure and increases the effective thickness of the top layer, "D". The height of the thermal bump is proportion to the square of the thickness of the top layer so modest

penetrations of the thermal gradient into the fin structure will generate large changes in the height of this distortion. This is the same effect that one sees in dependence of the peak values for the thermal profile on flow rate in Fig. 12.

No matter how high the value of "h" is made through good cooling of the silicon crystal there will always be some bowing of the crystal and some height to the thermal bump unless an active way is found to correct the shape of the surface. The 10-channel crystal with its two levels of cooling channels is designed to accomplish this type of active control of the diffraction surface of the crystal.[7] By raising the temperature of the cooling fluid in the lower channels above that flowing in the upper channels, one can make the upper surface concave and actively compensate for the bowing and for the thermal bump. This effect is illustrated in Fig. 15. This effect was demonstrated with the 10-channel crystal during the ANL/CHESS undulator run.[7] Fig. 16 compares the counting rate observed for the 10-channel crystal with and without a difference in temperature, "ΔT", between the two sets of cooling channels as a function of storage ring current. The temperature difference must be adjusted at each value of the beam current to obtain the maximum counting rate. More details of this experiment are given in the poster session paper No. A111 of this conference.[7]

Although considerable progress has been made and much has been learned about the art of cooling silicon crystals with liquid metals, much more needs to be done before the next generation of synchrotrons comes on line. Further experiments need to be performed to see just how thin the top layer of the crystal can be made before the crystalline planes become distorted and to demonstrated how much improvement is possible with increased flow of the cooling fluid. Experiments with the two levels of cooling channels will also

be most interesting. The latest version of this experiment uses film resistors on the back surface of the crystal to apply heat to the back of the crystal in place of the second level of cooling channels. This opens up the possibility of much greater control of the diffraction surface of the crystal than can be obtained with the two sets of cooling channels.

ACKNOWLEDGMENTS

The authors wish to thank P. J. Viccaro and D. M. Mills of ANL for many helpful discussions. This work was supported by the Department of Energy, BES-Materials Science, under contract No. W-31-109-ENG-38.

REFERENCES

1. R. K. Smither, G.A. Forster, C.A. Kot, T.M. Kuzay, Nucl. Instr. & Meth., A266, 517(1988)

2. W. R. Edward, E. H. Hoyer and A. C. Thompson, SPIE, 582, 281 (1985).

3. "Heat, Mass and Momentum Transfer," Chapters 5-11, W. M. Rohsenow and H. Y. Choi, Prentice-Hall, Inc., Englewood Cliffs, NJ, 1961. "Heat Transfer," A. J. Chapman, MacMillan Publishing Co., New York, NY, Chapters 5-13, 1974.

4. D. Bilderback, B. Batterman, M. Bedzyk, K. Finkelstein, C. Henderson, A. Merlini, D. Mills, Q. Shen, G. Shenoy, R. Smither, J. Viccaro, F. James, K. Robinson, and J. Slater, "The performance of a Hard X-ray Undulator at CHESS", Proceedings of the 3rd International Conference on Synchrotron Radiation Instrumentation, edited by M. Ando, Rev. Sci. Instrum. __, __, (1989).

5. D. Bilderback, C. Henderson, J. White, R. K. Smither and G.A. Forster, paper A088, "Undulator Heat Loading on X-ray Monochromators Cooled with Liquid Gallium", Proceedings of the 3rd International Conference on Synchrotron Radiation Instrumentation, edited by M. Ando, Rev. Sci. Instrum. __, __, (1989).

6. D. Bilderback, "Fabricating Rectangular Internal Cooling Channels in Silicon X-ray Monochromator Optics", Proceedings of the 3rd International Conference on Synchrotron Radiation Instrumentation, edited by M. Ando, Rev. Sci. Instrum. __, __, (1989).

7. R. Smither, "Variable Focus Crystal Diffraction Lens", Proceedings of the 3rd International Conference on Synchrotron Radiation Instrumentation, edited by M. Ando, Rev. Sci. Instrum., __ , __ (1989).

Table 1

Comparison of fluid properties of Ga and H_2O. Figure of merit = $C_v x \nu$

	Gallium	H_2O
Density (g/cc)(40°C)	6.1	1.0
Melting Point (°C)	29.8	0.0
Boiling Point (°C)	2205.	100.
Vapor Pressure (mmHg)(100°C)	10^{-10}	760.
Thermal Conductivity (W/cm,°C)	0.41	0.0068
Vol. Heat Capacity (Joules.cc,°C)	2.2	4.2
Viscosity (cp) (40°C)	1.6	1.0
Kinetic Viscosity (cp/g/cc)	0.27	4.2
Figure of Merit (Vol. Heat Cap. x Kin. Viscosity)	0.90	0.029

FIGURE CAPTIONS

Fig. 1. Plot of the count rate in the photon beam diffracted by the second crystal in the two crystal monochromator when one uses the standard CHESS side-cooled crystal with the full beam of the 6-pole wiggler verses the electron beam current in the storage ring.

Fig. 2. Schematic drawing of the 2-crystal monochromator showing the effects of the photon beam heating of the first crystal.

Fig. 3. A comparison of the rocking curves for the second crystal in the 2-crystal monochromator when the first cryston in the monochromator is the standard CHESS side-cooled crystal, for different electron beam currents in the storage ring.

Fig. 4. Schematic drawing of the different thermal distortions of a diffraction crystal subject to high heat loads from synchrotron beams.

Fig. 5. Plot of "h", the transfer coefficient, for liquid Ga (upper curve) and for water (lower curve) as a function of cooling fluid flow rate in a 0.5 dia. channel.

Fig. 6. Drawings of the cross sections of the three cooled silicon crystals used in the wiggler experiments.

Fig. 7. Plot of the surface temperature profile in the direction of the beam for the three different cooled silicon crystals used in the wiggler experiments.

Fig. 8. Plot of the rocking curves obtained with the three different silicon crystals in the wiggler experiments (photon energy of 20 keV, electron current of 46mA).

Fig. 9. Plots of rocking curves for the 5 channel crystal for different thicknesses of the stepped carbon filter in the photon beam.

Fig. 10. The thermal profile of the undulator beam superimposed on the cross section of the the slotted silicon crystal with the thin top layer. The side view and front view are crossed by lines at heights that correspond to the thermal isomers shown in the top view.

Fig. 11. Plot of the peak temperature of the thermal profile as a function of the rate of flow of the cooling fluid for the slotted crystal.

Fig. 12. The thermal profile of the undulator beam superimposed on the cross section of the the 10-channel crystal. The side view and front view are crossed by lines at heights that correspond to the thermal isomers shown in the top view.

Fig. 13. Plot of the FWHM of the rocking curves of the 10-channel crystal (circles) and the slotted crystal (triangles) for different diffraction energies and flow rates for the cooling fluid (Ga), as a function of the electron beam current in the storage ring.

Fig. 14. Plot of the counting rate in the photon beam from the monochromator verses the electron beam current, for the slotted crystal (triangles), the 10-channel crystal (circles) and the standard CHESS side-cooled crystal (squares), with different flow rates for the cooling fluid.

Fig. 15. Schematic drawing of the 10-channel crystal with two different temperatures of cooling fluids flowing in the two different sets of cooling channels, with T2 > T1. This generates a concave surface on the top of the crystal.

Fig. 16. A comparison of the count rate in the photon beam from monochromator verses electron beam current, for the 10-channel crystal with and without a temperature difference (ΔT) between the upper and lower cooling channels.

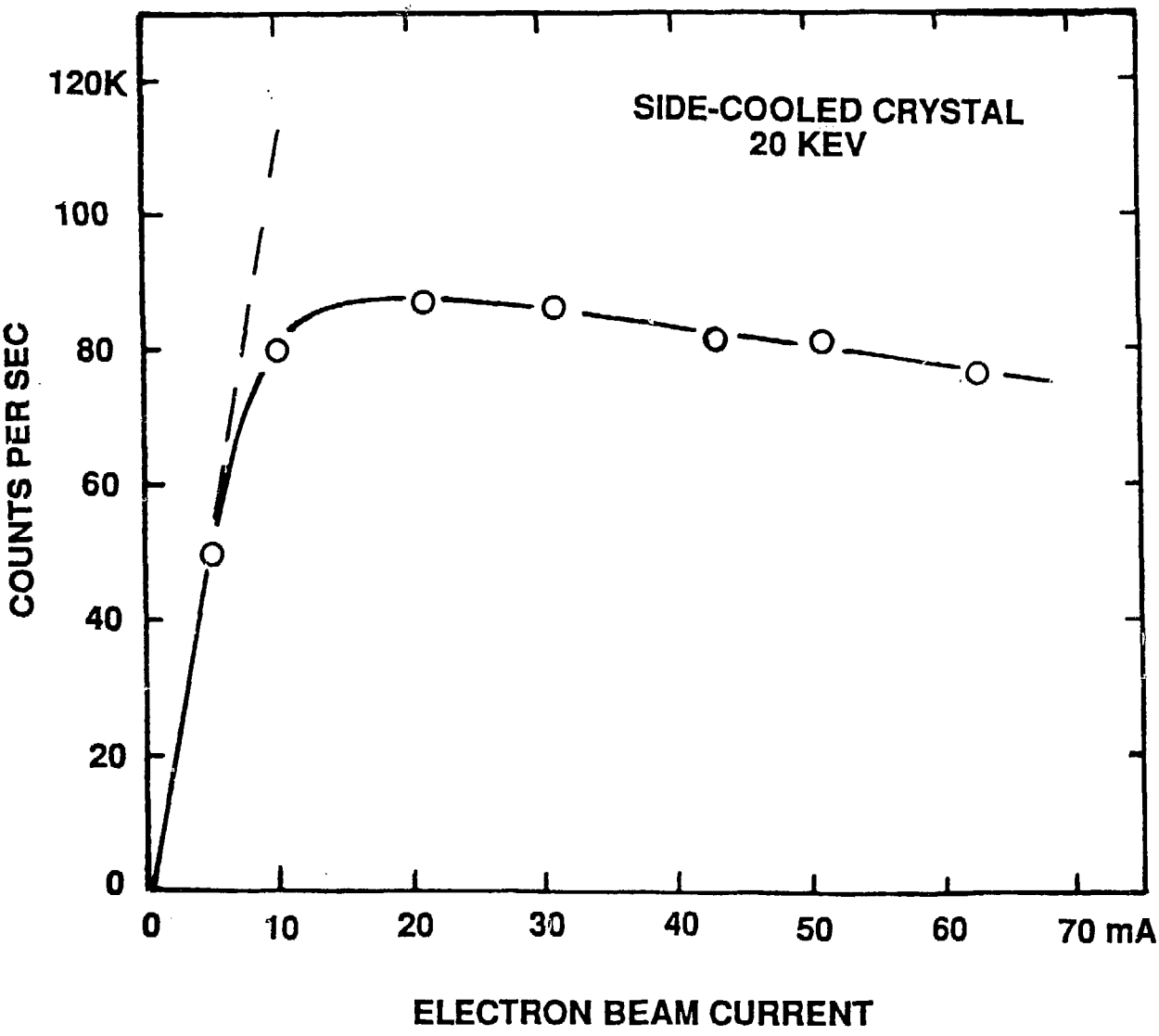
SIDE-COOLED CRYSTAL
20 KEV
120K
100
80
60
40
20
0
COUNTS PER SEC
0
10
20
30
40
50
60
70 mA
ELECTRON BEAM CURRENT

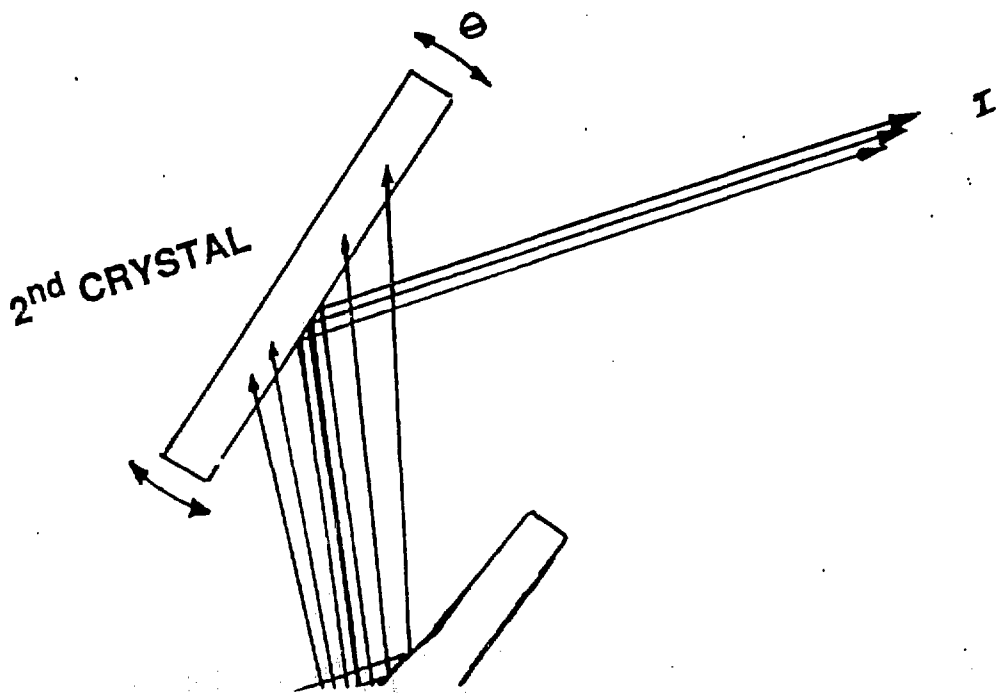
θ
I
2nd CRYSTAL

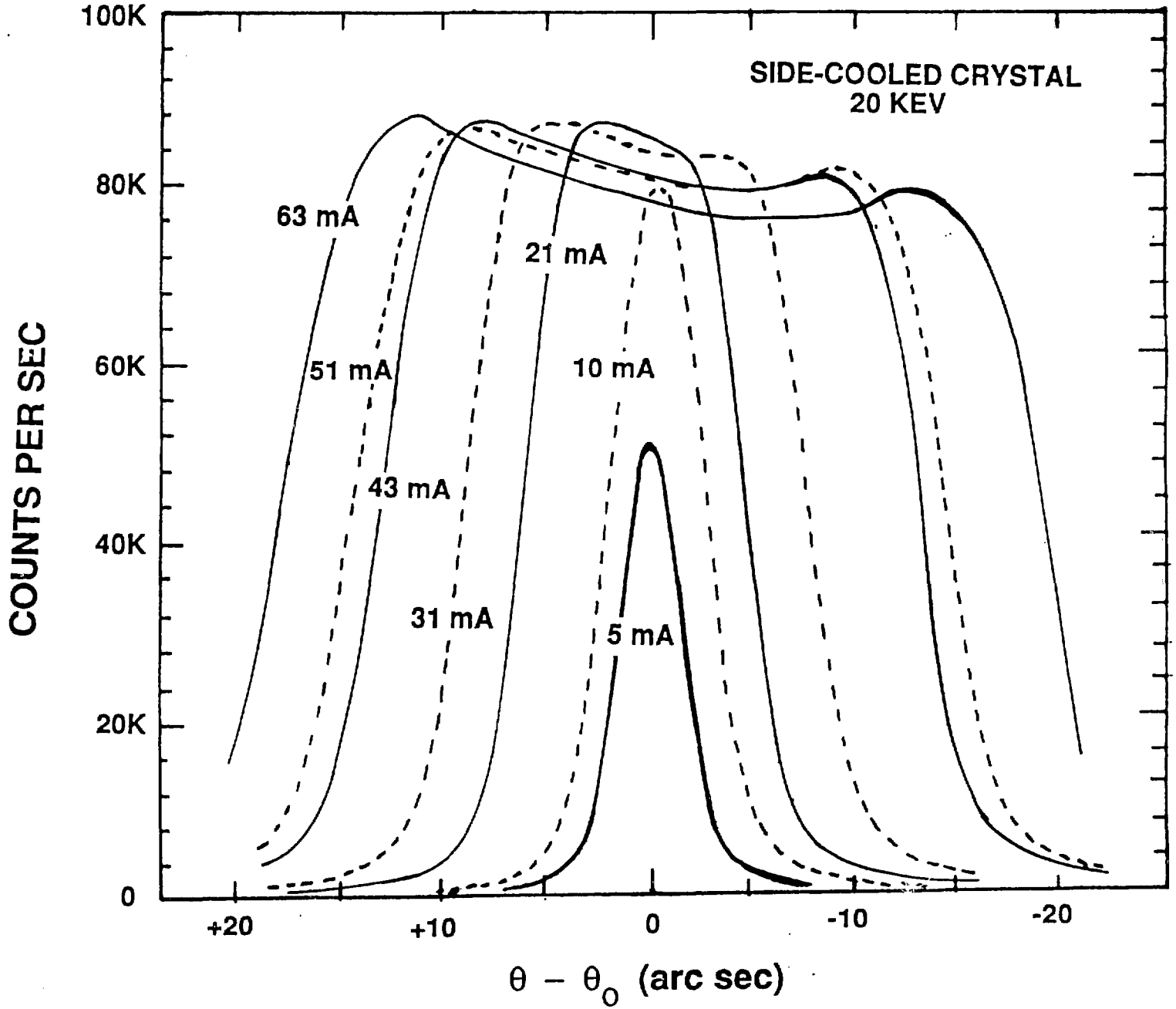
SIDE-COOLED CRYSTAL
20 KEV
63 mA
51 mA
43 mA
31 mA
21 mA
10 mA
5 mA
100K
80K
60K
40K
20K
0
COUNTS PER SEC
+20
+10
0
-10
-20
θ − θ0 (arc sec)

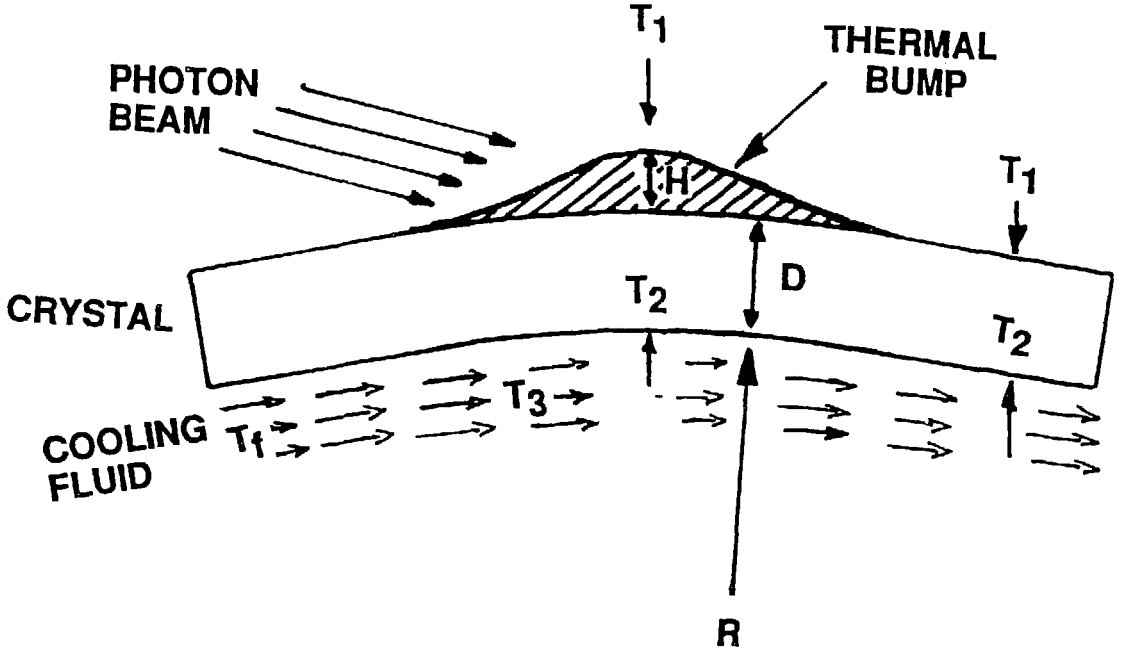
T1
THERMAL
BUMP
PHOTON
BEAM
H
T1
D
T2
CRYSTAL
T2
T3
COOLING
FLUID
Tf
R

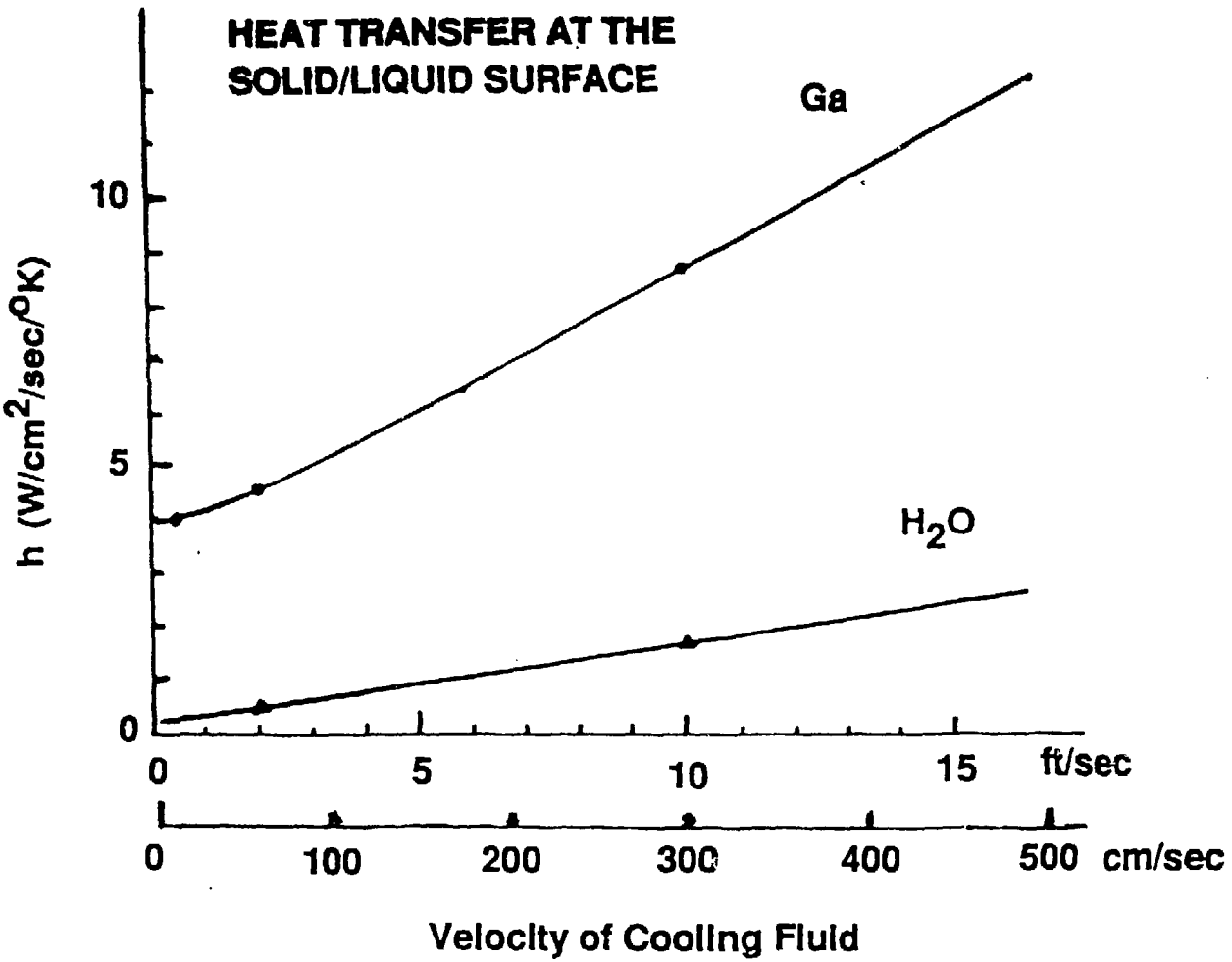
HEAT TRANSFER AT THE
SOLID/LIQUID SURFACE
Ga
H_2O
h (W/cm^2/sec/^{o}K)
10
5
0
0
5
10
15
ft/sec
0
100
200
300
400
500
cm/sec
Velocity of Cooling Fluid

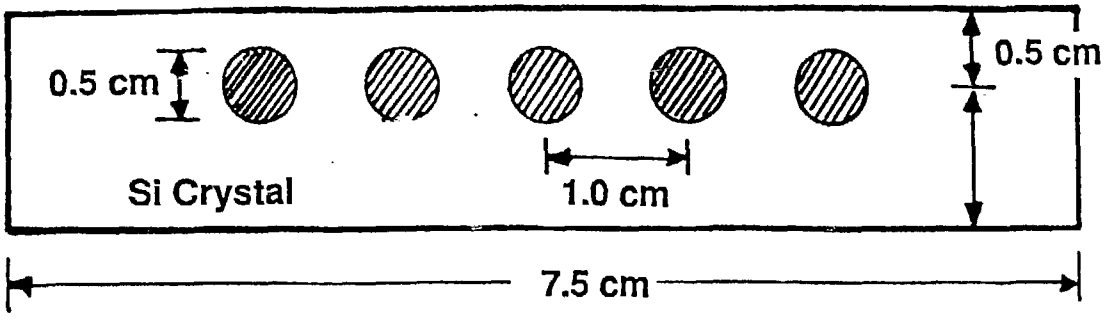
0.5 cm
0.5 cm
Si Crystal
1.0 cm
7.5 cm

a

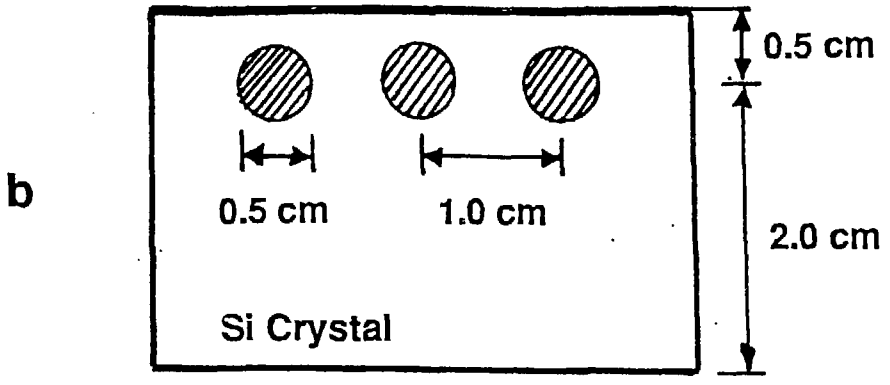
0.5 cm
0.5 cm
1.0 cm
2.0 cm
Si Crystal
3.8 cm

b

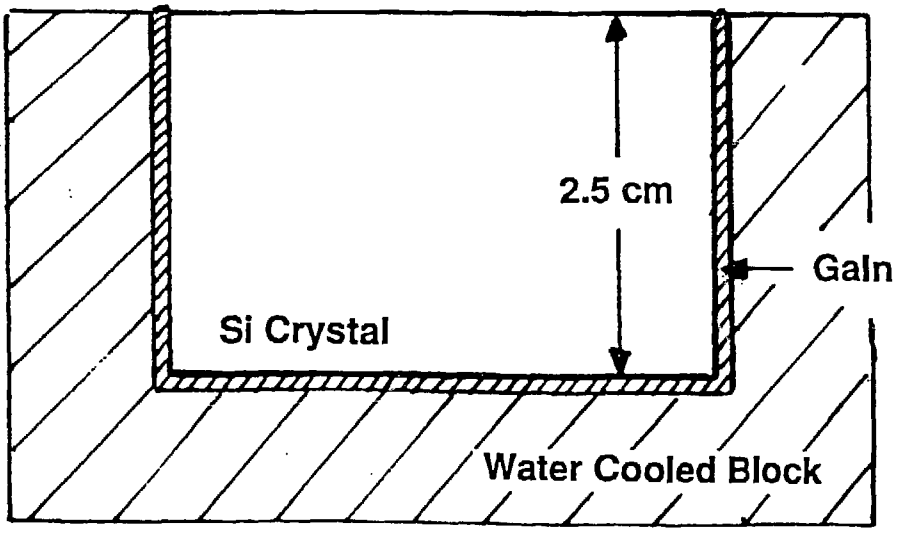
2.5 cm
Galn
Si Crystal
Water Cooled Block

c

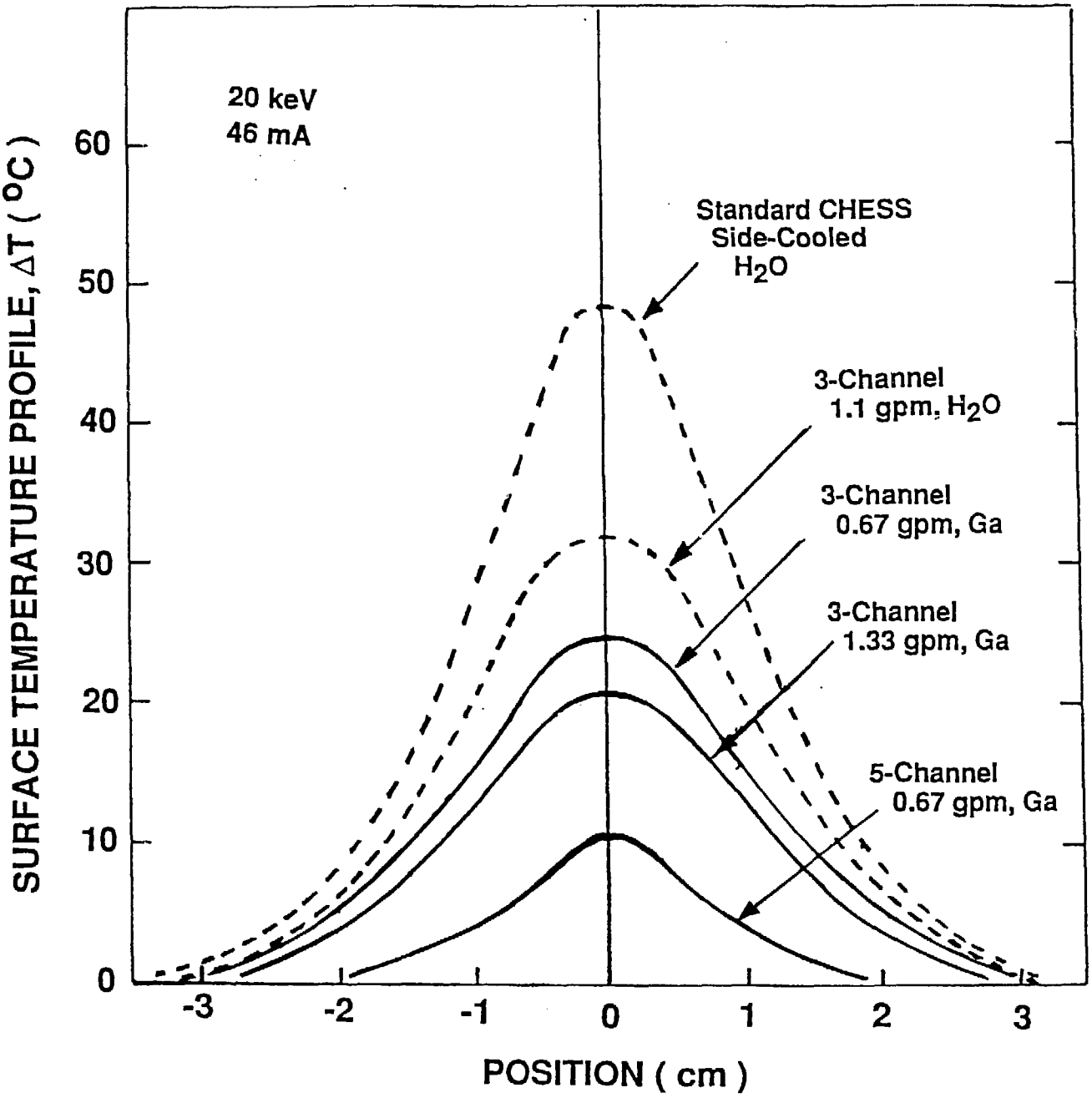
20 keV
46 mA
Standard CHESS
Side-Cooled
H_2O
3-Channel
1.1 gpm, H_2O
3-Channel
0.67 gpm, Ga
3-Channel
1.33 gpm, Ga
5-Channel
0.67 gpm, Ga
SURFACE TEMPERATURE PROFILE, ΔT (°C)
POSITION (cm)
0
10
20
30
40
50
60
-3
-2
-1
0
1
2
3

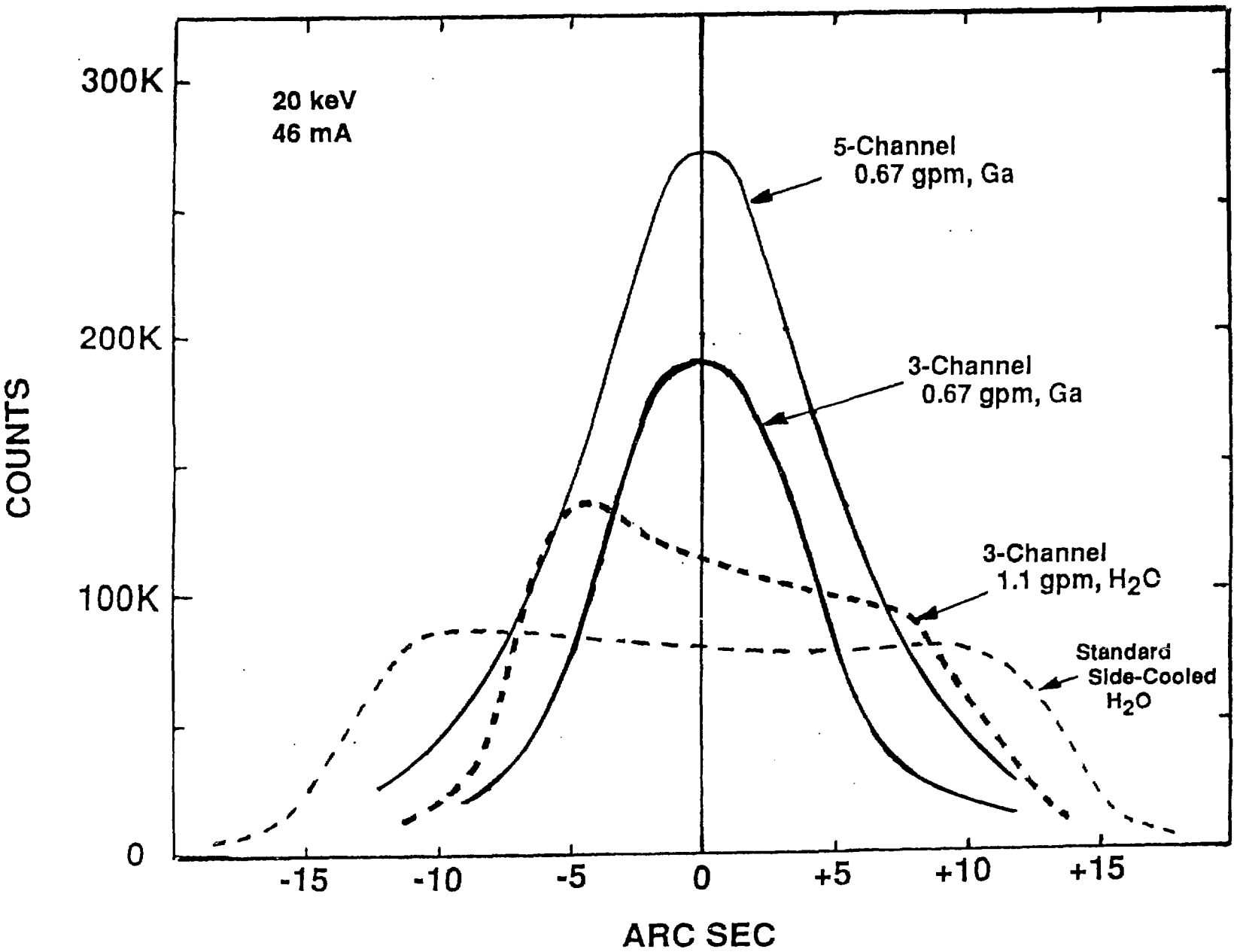
300K
200K
100K
0
COUNTS
20 keV
46 mA
5-Channel
0.67 gpm, Ga
3-Channel
0.67 gpm, Ga
3-Channel
1.1 gpm, H_2O
Standard
Side-Cooled
H_2O
-15
-10
-5
0
+5
+10
+15
ARC SEC

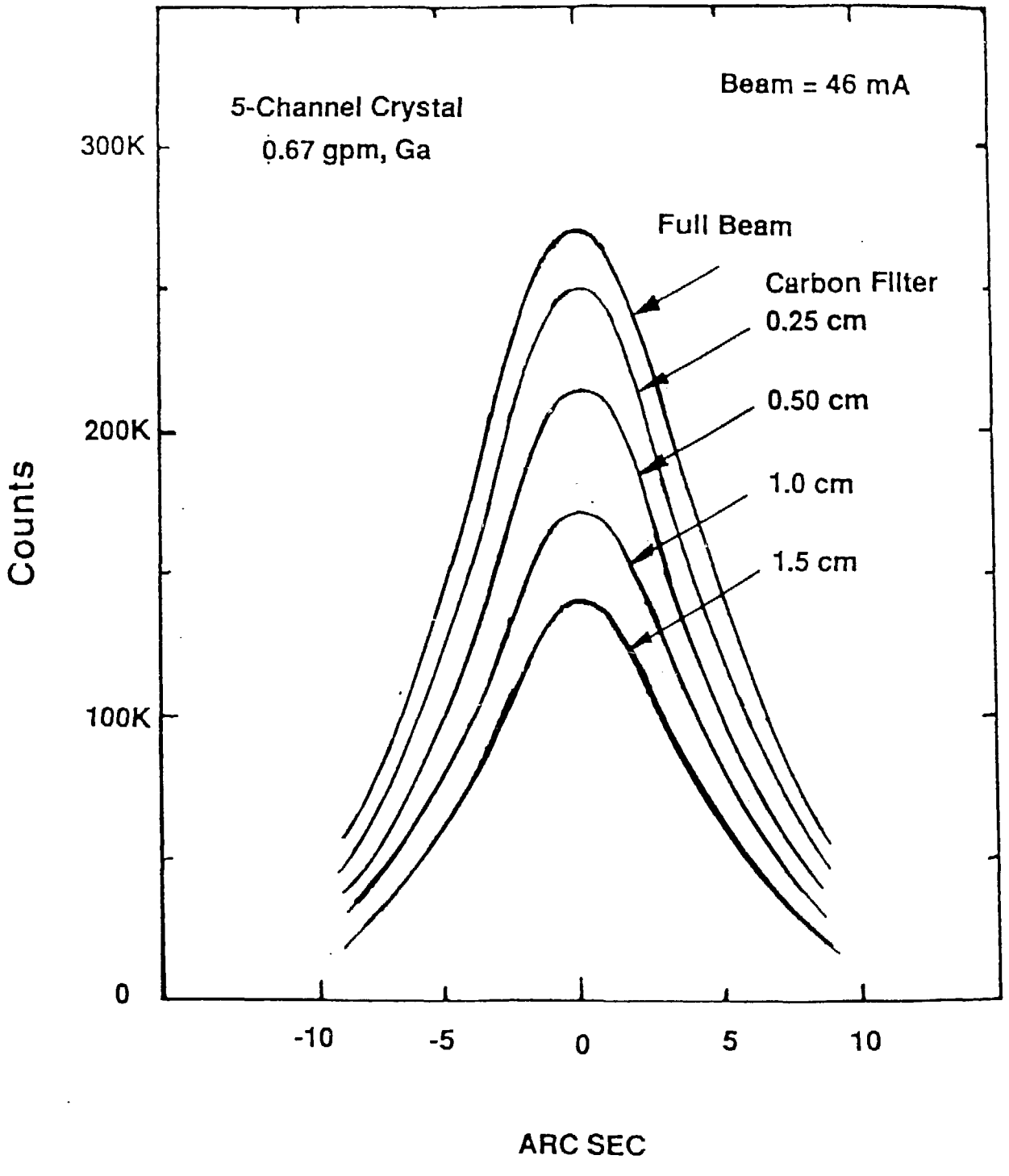
5-Channel Crystal
0.67 gpm, Ga
Beam = 46 mA
300K
200K
100K
0
Counts
Full Beam
Carbon Filter
0.25 cm
0.50 cm
1.0 cm
1.5 cm
-10
-5
0
5
10
ARC SEC

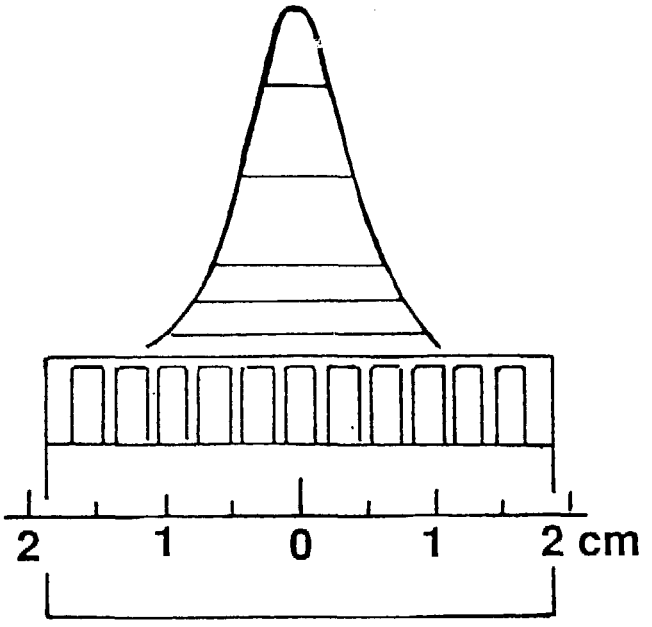
2
1
0
1
2 cm

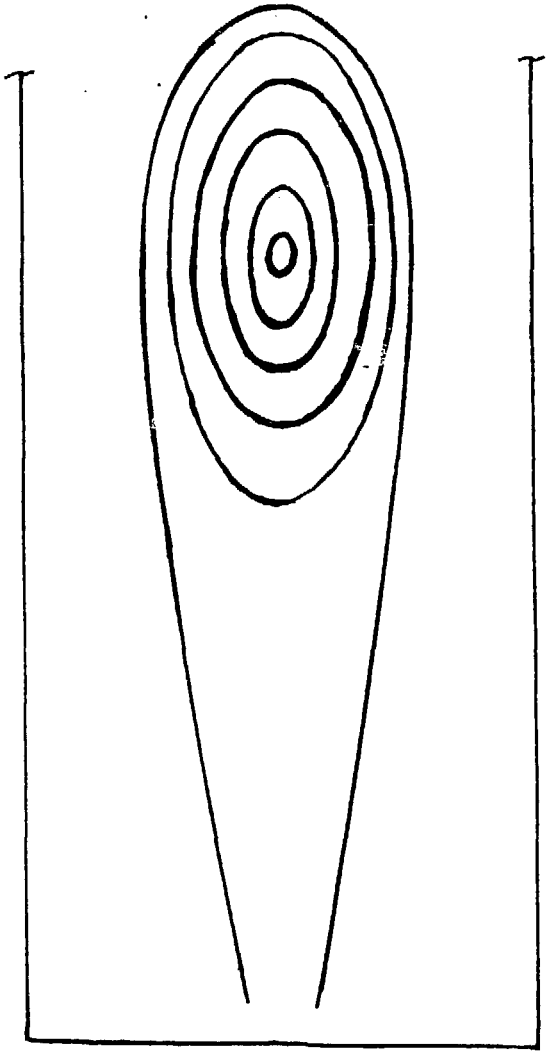

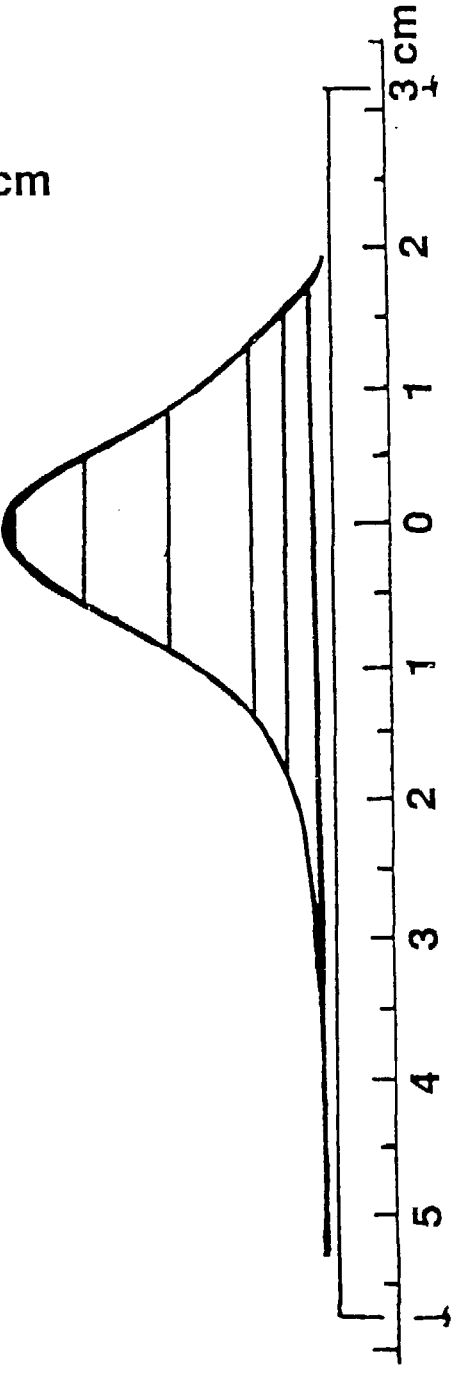
3 cm
2
1
0
1
2
3
4
5

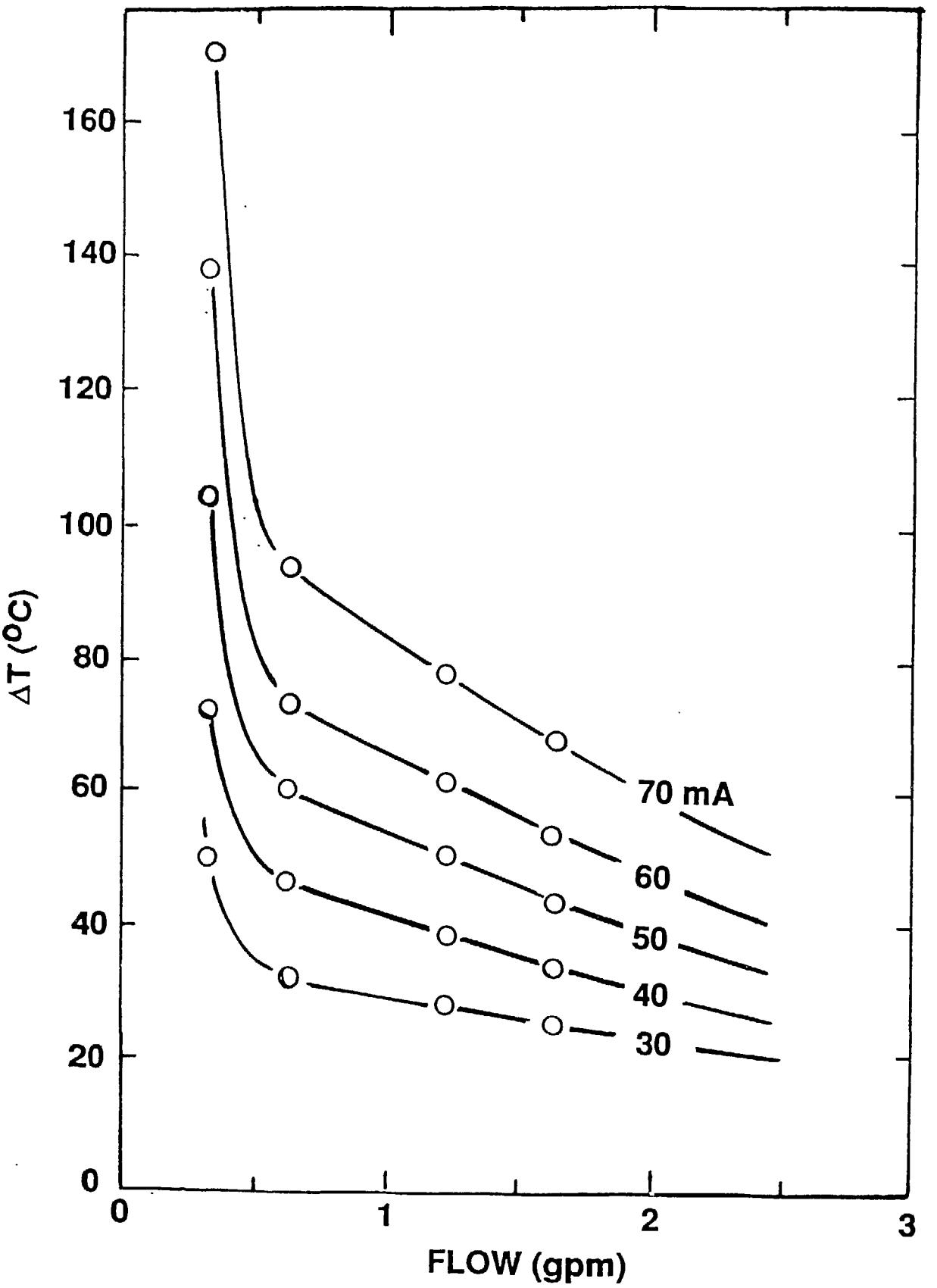
160
140
120
100
80
60
40
20
0
ΔT (°C)
0
1
2
3
FLOW (gpm)
70 mA
60
50
40
30

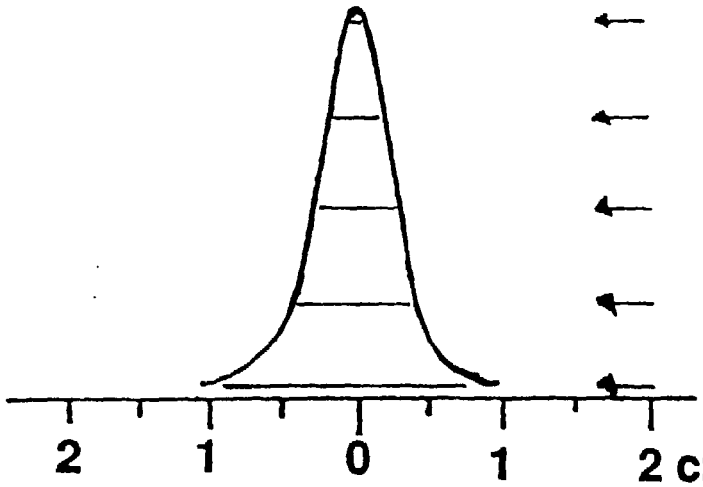

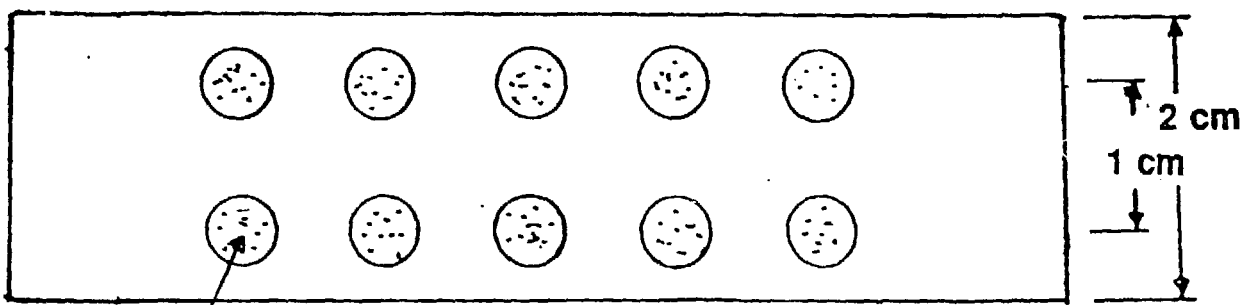

0.5 cm dia.
channel

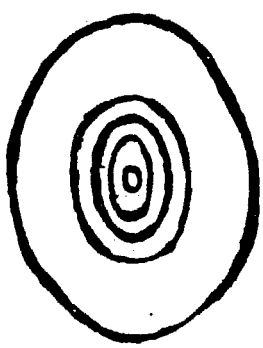

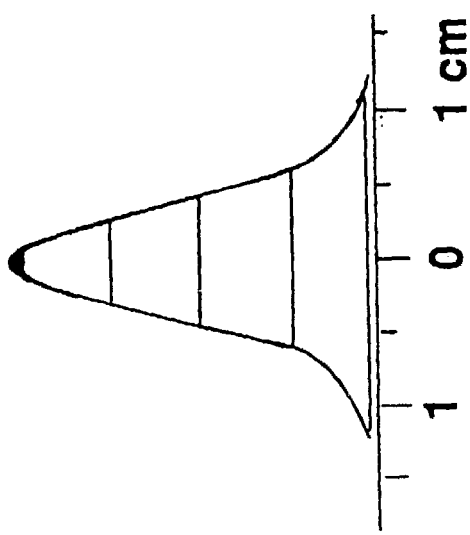

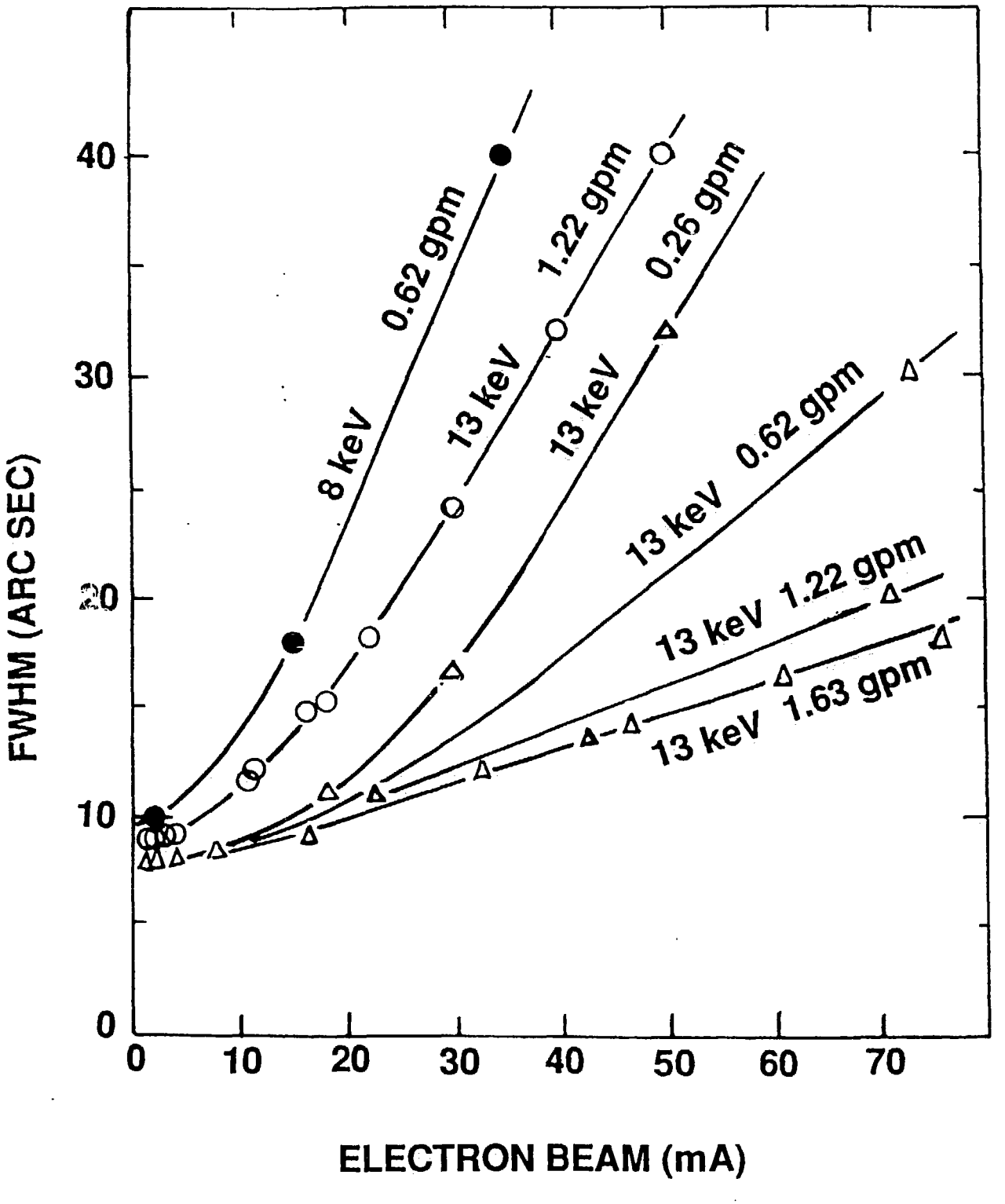
FWHM (ARC SEC)
ELECTRON BEAM (mA)
0
10
20
30
40
0
10
20
30
40
50
60
70
8 keV 0.62 gpm
13 keV 1.22 gpm
13 keV 0.26 gpm
13 keV 0.62 gpm
13 keV 1.22 gpm
13 keV 1.63 gpm

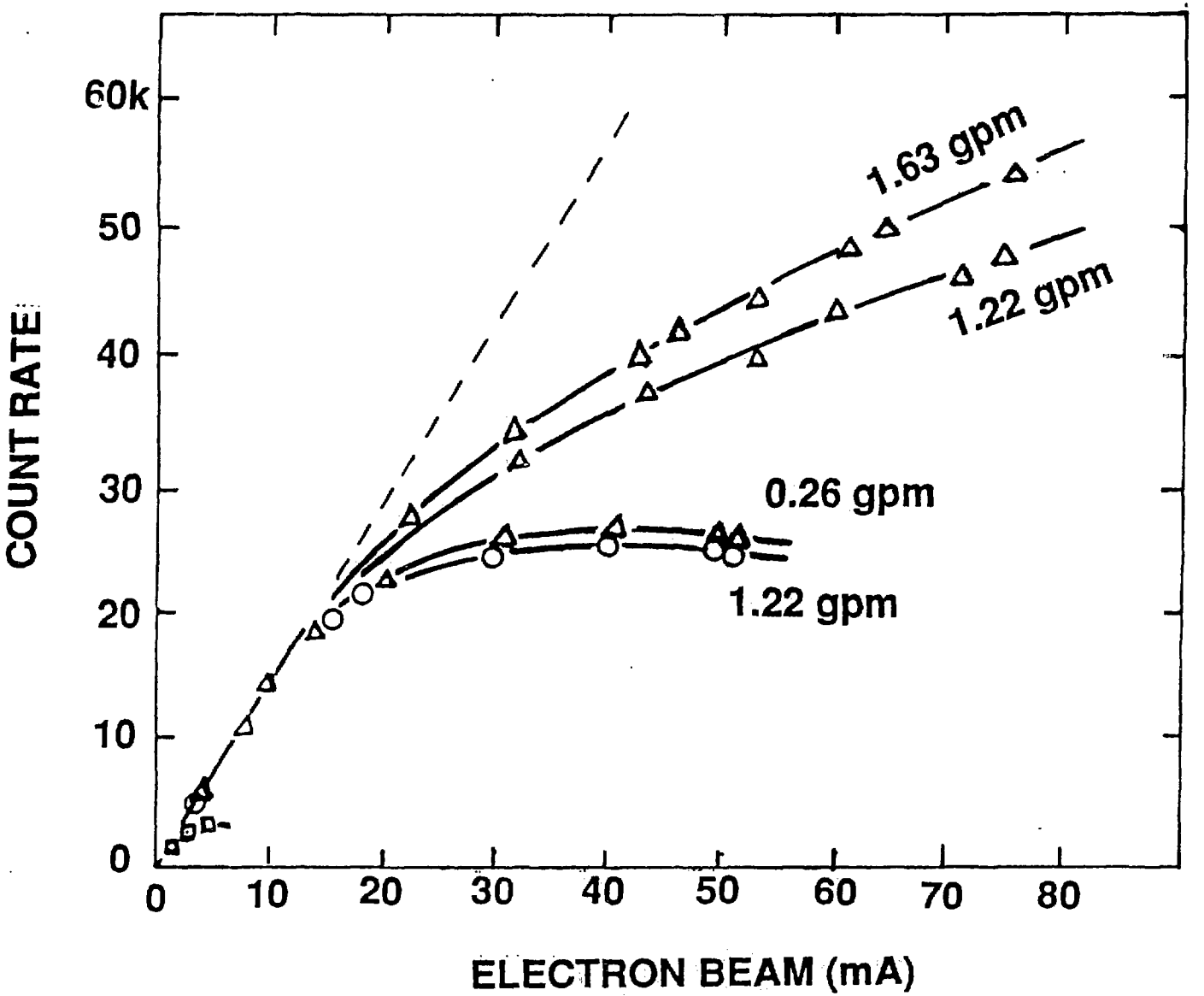
60k
50
40
30
20
10
0
COUNT RATE
0
10
20
30
40
50
60
70
80
ELECTRON BEAM (mA)
1.63 gpm
1.22 gpm
0.26 gpm
1.22 gpm

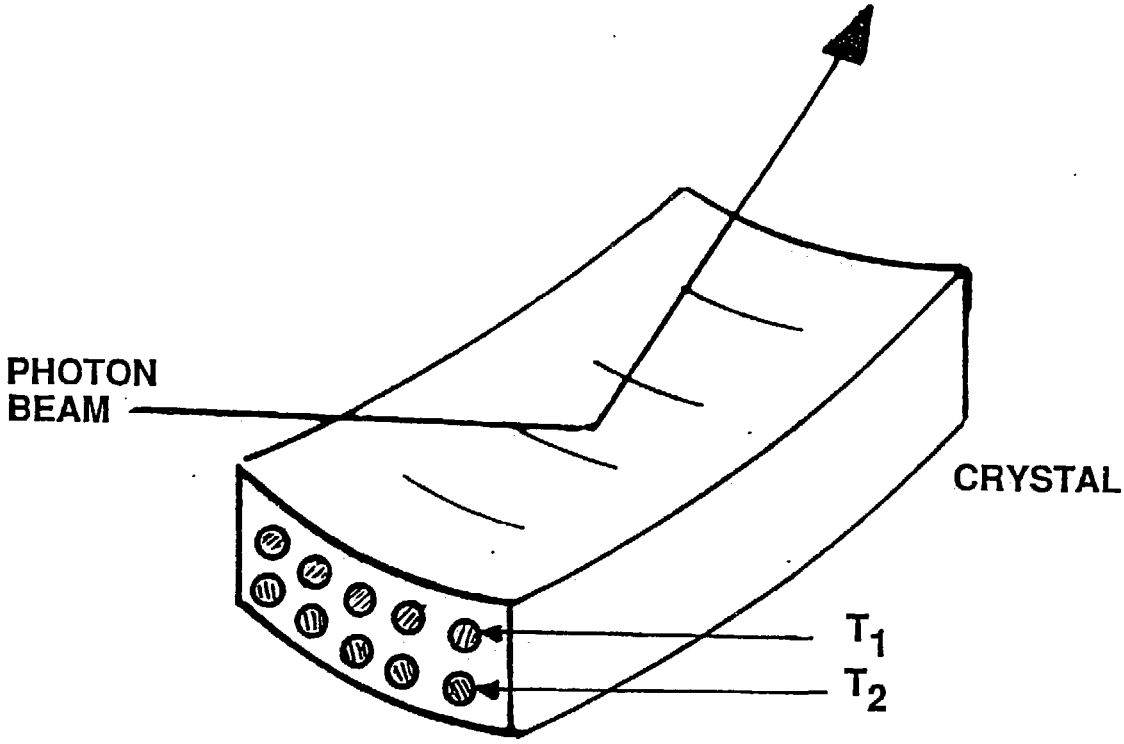
PHOTON
BEAM
CRYSTAL
T_1
T_2

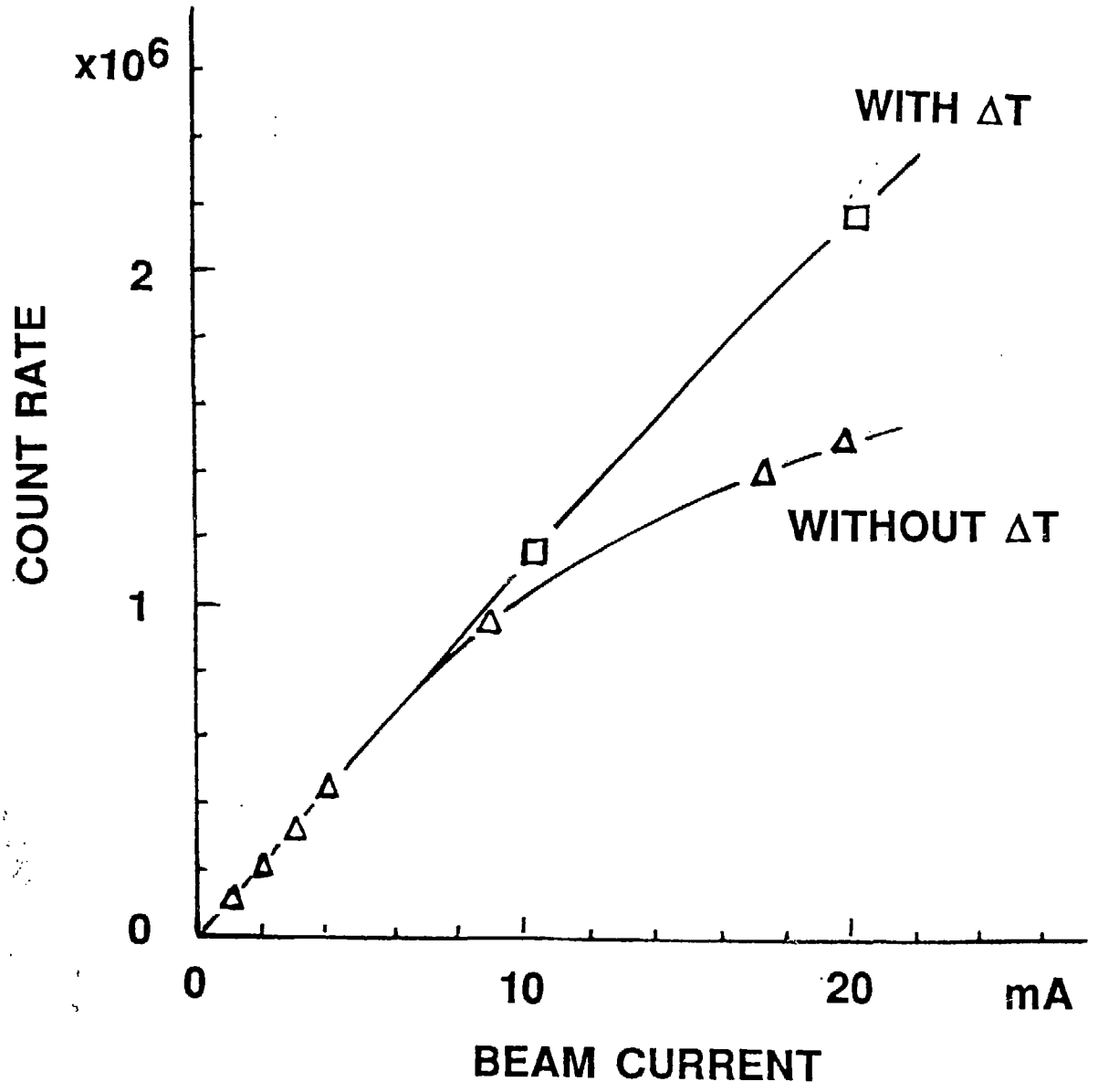
x10^6
2
1
0
COUNT RATE
WITH ΔT
WITHOUT ΔT
0
10
20
mA
BEAM CURRENT